ACS chemical biology

Articles

pubs.acs.org/acschemicalbiology

# Targeting and Maturation of Erv1/ALR in the Mitochondrial Intermembrane Space

Emmanouela Kallergi,[†,‡] Maria Andreadaki,[†,‡] Paraskevi Kritsiligkou,[†,‡] Nitsa Katrakili,[†] Charalambos Pozidis,[†] Kostas Tokatlidis,*[,†,§] Lucia Banci,*[,∥,⊥] Ivano Bertini,*[,∥,⊥] Chiara Cefaro,[∥,⊥] Simone Ciofi-Baffoni,[∥,⊥] Karolina Gajda,[∥] and Riccardo Peruzzini[∥]

[†]Institute of Molecular Biology and Biotechnology, Foundation for Research and Technology Hellas (IMBB-FORTH), Heraklion 71110, Crete, Greece

[‡]Department of Biology, University of Crete, Heraklion 71409, Crete, Greece

[§]Department of Materials Science and Technology, University of Crete, Heraklion 71003, Crete, Greece

[∥]Magnetic Resonance Center CERM, University of Florence, Via Luigi Sacconi 6, 50019 Sesto Fiorentino, Florence, Italy

[⊥]Department of Chemistry, University of Florence, Via della Lastruccia 3, 50019 Sesto Fiorentino, Florence, Italy

Supporting Information

**ABSTRACT:** The interaction of Mia40 with Erv1/ALR is central to the oxidative protein folding in the intermembrane space of mitochondria (IMS) as Erv1/ALR oxidizes reduced Mia40 to restore its functional state. Here we address the role of Mia40 in the import and maturation of Erv1/ALR. The C-terminal FAD-binding domain of Erv1/ALR has an essential role in the import process by creating a transient intermolecular disulfide bond with Mia40. The action of Mia40 is selective for the formation of both intra and intersubunit structural disulfide bonds of Erv1/ALR, but the complete maturation process requires additional binding of FAD. Both of these events must follow a specific sequential order to allow Erv1/ALR to reach the fully functional state, illustrating a new paradigm for protein maturation in the IMS.

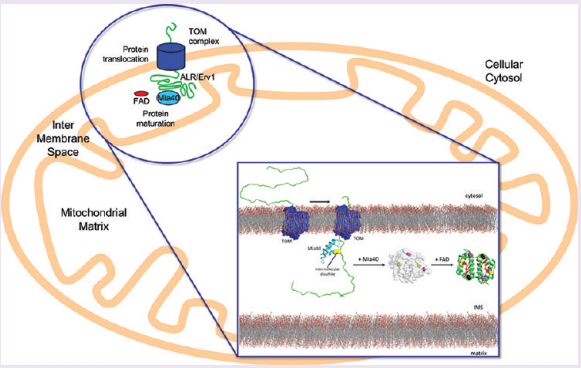


The mitochondrial intermembrane space (IMS) contains a large share of proteins having disulfide bonds in their functional state.[1,2] All of these proteins are nuclear encoded and must be imported and then trapped in the IMS.[3] Mechanistically distinct import pathways have been described for different classes of IMS proteins.[4] Most IMS proteins do not contain the canonical N-terminal mitochondrial targeting sequence (used primarily for targeting to the matrix), and their IMS-accumulation requires their specific folding in the IMS.[5] The folding is usually triggered by the acquisition of cofactors and/or by intramolecular disulfide bridges.[5] According to the proposed folding trap hypothesis, the folded state prevents back-translocation out of the mitochondria and thereby confers unidirectional import of these proteins. Recently, a disulfide relay system has been identified in the IMS,[6] involving two proteins: the FAD-dependent sulfhydryl oxidase Erv1/ALR (yeast and human homologues, respectively) and the mitochondrial IMS assembly protein Mia40. This redox system traps polypeptide substrates containing conserved cysteines in the IMS through an oxidative folding process. The general consensus supports a model whereby the substrates are oxidized and folded by Mia40, which introduces disulfide bonds into them.[7,8] Reduced Mia40 is then oxidized back through a process in which electrons are transferred from the reduced active CPC site of Mia40 to Erv1/ALR. The reoxidation step of Mia40 has been recently investigated in detail and has been shown to be mediated directly and exclusively by a CXXC motif of Erv1/ALR located in an unstructured N-terminal domain.[9−14] Specifically, recognition of the reduced Mia40 active site depends on a specific 12aa stretch in this N-terminal domain that interacts with Mia40 *via* hydrophobic interactions following a substrate-mimicry mechanism.[13] These studies[10,13] conclusively showed that this N-terminal Erv1/ALR region is necessary and sufficient for this interaction.

The interaction of Erv1/ALR and Mia40 is, however, rather complex as it can occur in a further, drastically different circumstance. This second facet of the interaction of Erv1/ALR with Mia40 occurs in the process of import of Erv1/ALR, during which Erv1/ALR is recognized by Mia40 as an import substrate of the Mia pathway.[15,16] This step of the interaction between Erv1/ALR and Mia40 is crucial for the biogenesis and maturation of Erv1/ALR, as it is the prerequisite for its biological function as oxidoreducatse. The comprehension at

**Received:** November 22, 2011
**Accepted:** January 18, 2012
**Published:** February 1, 2012

   dx.doi.org/10.1021/cb200485b | *ACS Chem. Biol.* 2012, 7, 707−714

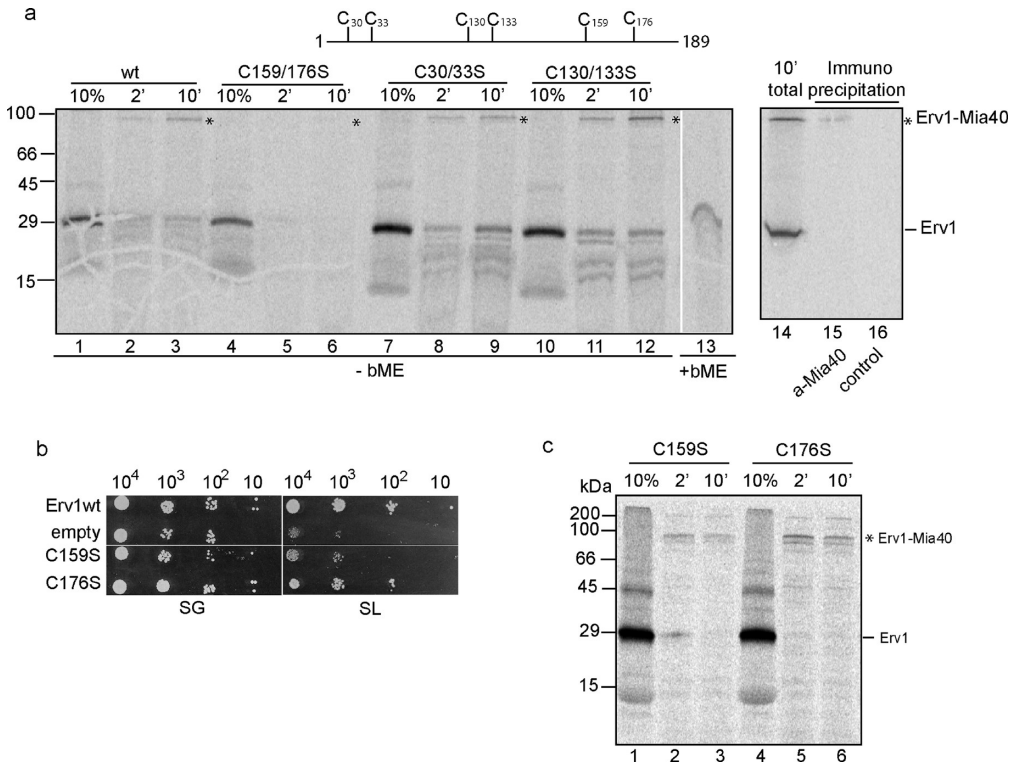


**Figure 1.** The Erv1 C-terminal structural cysteine pair is crucial for docking to Mia40. (a) Schematic representation of Erv1 cysteines and import of radioactive wild-type (wt) and double cysteine mutants of Erv1 in wt mitochondria monitored by SDS-PAGE and autoradiography. The intermediate with endogenous Mia40 is shown by an asterisk, 10% represents the fraction of the total amount of *in vitro* translated material used for import, and 2′ and 10′ represent time (minutes) of import. In lane 13, $\beta$-mercaptoethanol ("bME") was added in the sample buffer before SDS-PAGE. Lanes 15 and 16: immunoprecipitation of the import mixture of wt Erv1 after 10 min of import (shown in lane 14 before immunoprecipitation) was performed with either rabbit anti-Mia40 antisera (lane 15) or with control preimmune antisera (lane 16). (b) *In vivo* yeast complementation assay for GalErv1 *S. cerevisiae* cells supplemented with a plasmid expressing wt Erv1, the C159S mutant, C176S mutant, or no gene at all (empty). Four serial dilutions were spotted on plates with either galactose (SG) and lactate (SL) plus 0.2% glucose containing media. (c) Import of radioactive single cysteine mutants C159S and C176S of Erv1 in wt mitochondria and their capacity to form the intermediate with endogenous Mia40 (as in panel b).

the molecular level of this recognition process will contribute to understand how Erv1/ALR protein manages the two different types of interactions with Mia40.

Erv1/ALR exist as homodimers where each subunit contains, in the FAD-binding structural domain, a disulfide bond (a so-called proximal disulfide) in redox communication with the FAD moiety.[13,17−19] A further disulfide bond in the unstructured N-terminal domain is involved in electron shuttling (distal disulfide), and a third one in the FAD-binding, C-terminal domain has a structural role (structural disulfide). ALR has a further disulfide bond (two per dimer) connecting the two subunits, also having a structural function. As a consequence of the inefficiency of ALR to be imported in yeast mitochondria,[20] Erv1 has been used here (as in all previous studies) for mitochondrial import studies. For the molecular characterization of the maturation mechanism, we used the human homologue ALR (43% sequence identity with Erv1), in which the two nonconserved Cys154 and Cys165 that do not affect its function were mutated to Ala.[13,14,21] On the basis of import assays, biochemical, biophysical, and structural analyses, we present here a mechanistic model for the Mia40-dependent import and maturation of Erv1/ALR. It is shown that this process depends on structural determinants of Erv1/ALR (not involved in its enzymatic activity), on the interaction with Mia40 and on FAD binding. This study illustrates a new paradigm of a precisely concerted mechanism requiring both Mia40 and FAD for the maturation of Erv1/ALR in the IMS.

## RESULTS AND DISCUSSION

**Mitochondrial Import of Erv1.** Import experiments with isolated yeast mitochondria and radioactive versions of Erv1 translated *in vitro* showed that the C30/33S and the C130/133S mutants were imported at the same level as the wild-type protein and gave a higher size radioactive band when NEM was added in the import reaction as a means to stabilize putative intermediates with endogenous Mia40 (indicated by an asterisk in Figure 1a, lanes 1−3 for wild-type, lanes 7−9 for the C30/33S mutant, and lanes 10−12 for the C130/133S mutant). The size of this band is compatible with an adduct of imported Erv1 with endogenous Mia40 and was $\beta$-mercaptoethanol (bME)-sensitive (Figure 1a, lane 13). Additionally, when the total import mixture of wild-type Erv1 after 10 min of import (lane 14) was immunoprecipitated, the intermediate was pulled down using specific anti-Mia40 antibodies (lane 15) but not with control preimmune antisera (lane 16). The above two controls (bME sensitivity and immunoprecipitation with anti-Mia40 antibodies) prove that this complex is a transient intermediate between imported Erv1 and endogenous Mia40. By contrast, the C159/176S mutant was strikingly incapable of import (Figure 1a, lanes 4−6) in the same import assay (using the same batch of mitochondria and the same conditions as wild-


dx.doi.org/10.1021/cb200485b | ACS Chem. Biol. 2012, 7, 707−714

type Erv1). It was therefore clear that the double mutant C159/176S displayed a substantial import defect in isolated mitochondria. Complementation assays in yeast cells using a Gal-Erv1 strain[10] supplemented with different versions of His-tagged Erv1 mutants and all expressed under the same promoter showed that the C159S or the C176S mutant are strongly affected (Figure 1b) but still viable,[22,23] while the wild-type as a control restored viability. This effect could be attributed to either defective import *in vivo* or enhanced *in vivo* degradation of the mutants or a combination of the two. As our efforts to assess the levels of Erv1 mutant proteins by Western blots were inconclusive, these possibilities remain open. We then further analyzed the behavior of the single point mutants C159S and C176S in import assays. Both mutants were affected in their import compared to the wild-type (Figure 1c): C159S is mostly affected in the formation of the intermediate with Mia40, while C176S gives a higher percentage of the intermediate with Mia40 but essentially no release of Erv1 from Mia40 (Figure 1c). This behavior is reminiscent of the import of other Mia40 substrates where mutation of the docking Cys substantially affects the formation of the intermediate with Mia40, while mutation of the partner Cys results in a "stuck" intermediate, since the reaction cannot proceed after binding to Mia40.[24] Taken together, these data (Figure 1) show that Cys159 is the docking cysteine for Erv1 to Mia40 and that the C-terminal part of Erv1 interacts with Mia40 during its import.

A construct lacking the first 72 amino acids of Erv1 (called ΔN72 Erv1 which retains only the FAD-binding structural domain of Erv1) was imported at the same levels as the wild-type full-length protein and also formed the intermediate with Mia40 (Figure 2a). Even ΔN133 (lacking 133 of the total 189 amino acids, *i.e.*, 70% of the Erv1 sequence, Figure 2b) maintained the capacity to be imported into mitochondria and to interact with Mia40 (Figure 2c). This shows that the N-terminal part of Erv1 is not required for import in isolated mitochondria and that the FAD-binding domain retains enough information for translocation across the outer membrane and interaction with Mia40. To further delineate the minimal segment of Erv1 required to bind to Mia40, a C-terminal deletion, ΔC13, lacking the last 13 residues 177−189 after Cys176, was generated and imported in mitochondria without any observable effect on its import and interaction with Mia40. We observed that this construct seems mostly stuck in an intermediate with Mia40 (Figure 2d), suggesting that the C-terminal 13-residue tail may be involved in the release from Mia40 rather than the initial docking to Mia40. This deletion analysis therefore shows that the minimal segment of Erv1 required for docking to Mia40 is the segment between residues 134−176 within the FAD-binding domain.

**Maturation Mechanism of ALR.** To reproduce *in vitro* the IMS-imported ALR state, we produced a fully reduced, FAD-free state of the C-terminal domain of ALR (sf-ALR hereafter; see Supplementary Methods for details). Gel-filtration data and static multiangle light scattering measurements indicate that the protein in this state is dimeric at 100 $\mu$M protein concentrations (Supplementary Figure 1). Circular dichroism spectra show that the protein loses 25% of its $\alpha$-helical content with respect to the mature form (Figure 3a). $^{1}H-^{15}N$ HSQC NMR spectra showed some chemical shift dispersion, at variance with what occurs in a completely unfolded protein state, indicating the presence of some degree of tertiary structural organization, but still rather limited with respect to

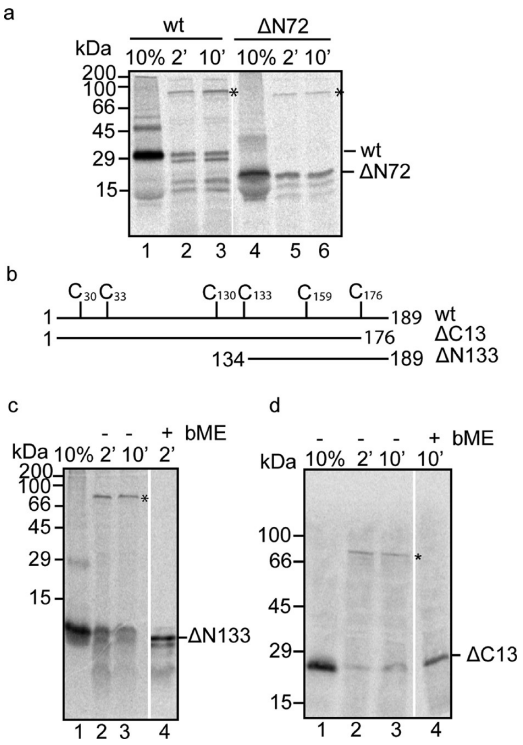


**Figure 2.** The C-terminal FAD-core of Erv1 drives interaction with Mia40. (a) Import of radioactive wild-type (wt) and ΔN72 Erv1 in wt mitochondria (as in Figure 1a) and their capacity to form the intermediate with endogenous Mia40 (shown by an asterisk). (b) Schematic representation of Erv1 wt and deletion mutants ΔN133 and ΔC13. (c) Import of radiolabeled precursors of ΔN133. The Erv1-Mia40 intermediate is shown by an asterisk, and $\beta$-mercaptoethanol treatment is indicated ("bME"). (d) As in panel c, for import of the ΔC13 deletion mutant.

that observed for the folded FAD-bound state of sf-ALR (Figure 3b). Long stretches at the N- and C-termini experience conformational flexibility typical of completely unfolded proteins, as monitored by heteronuclear relaxation rates and $^{15}N\{^{1}H\}$-NOEs (Supplementary Table 1). The chemical shift index analysis indicated that residues in those segments indeed do not have any secondary structure elements. In particular, the last $\alpha$-helix (helix $\alpha$5), present in the *E. coli*-purified sf-ALR, is completely lost (Figure 3c). The other assigned residues (Figure 3c), despite having some tertiary structure organization as indicated by relatively high heteroNOE values (Supplementary Table 1), are involved in extensive conformational exchange processes as monitored by high $R_2$ values (Supplementary Table 1). In conclusion, fully reduced FAD-free sf-ALR behaves in solution as a dimeric protein having a native-like secondary structure but with very limited static tertiary structure; it contains a completely flexible and unstructured C-terminal segment, compared to its well-ordered conformation in the *E. coli*-purified sf-ALR. Considering the ability of Mia40 to specifically recognize unstructured and flexible regions, the fluxional conformational state of the fully reduced FAD-free sf-ALR can be a suitable substrate for Mia40, despite its large molecular weight with respect to the most common Mia40-substrates,[16] which are smaller than <10 kDa and are completely unstructured.[8,25]

Addition of 2 equiv of fully oxidized Mia40 ($Mia40_{3S-S}$) to fully reduced $^{15}N$-labeled FAD-free sf-ALR did not produce large chemical shift changes in the $^{1}H-^{15}N$ HSQC map,


dx.doi.org/10.1021/cb200485b | *ACS Chem. Biol.* 2012, 7, 707−714

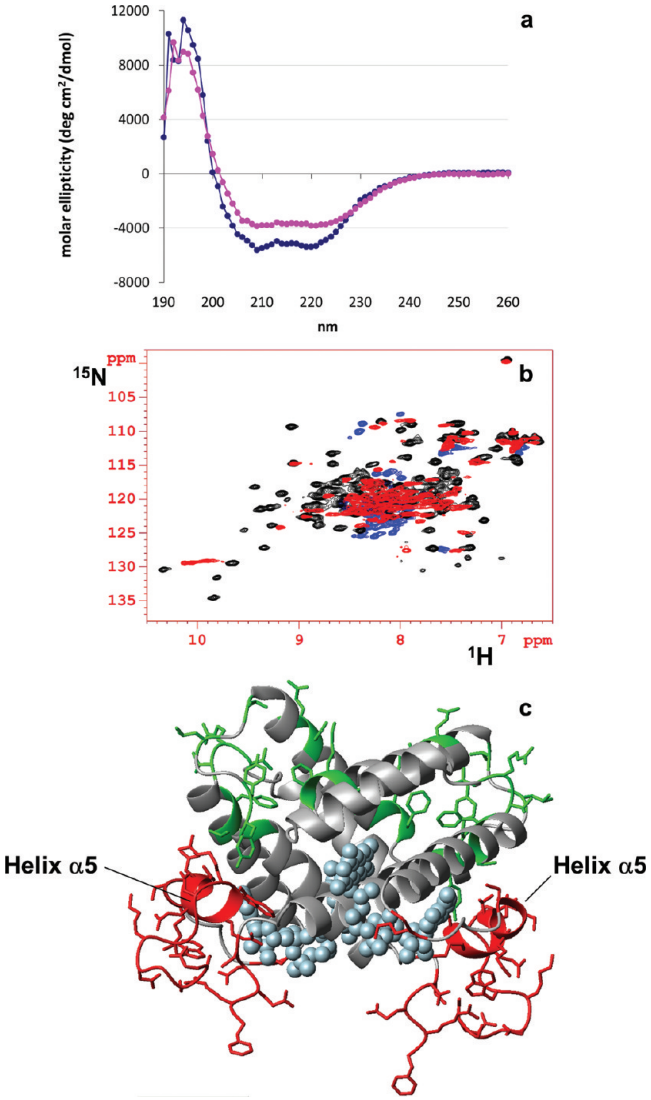


**Figure 3.** Structural-conformational properties of fully reduced FAD-free sf-ALR. (a) Circular dichroism spectra of fully reduced FAD-free sf-ALR (magenta ●) and of *E. coli*-purified sf-ALR state (blue ●). (b) Overlay of $^{1}H-^{15}N$ HSQC spectra of fully reduced FAD-free sf-ALR (in red), of *E. coli*-purified sf-ALR state (in black), and fully reduced apoCox17 (in blue) taken as an example of a HSCQ map of a completely unfolded protein state. (c) Residues showing backbone flexibility typical of a completely unfolded protein (motions in the ns−-ps time scale) and residues showing extensive conformational exchange processes (motions in the ms−$\mu$s time scale) are mapped in red and green, respectively, on the ribbon representation of *E. coli*-purified sf-ALR state. FAD is in light blue, and helix $\alpha$5, which is completely lost in the fully reduced FAD-free sf-ALR state, is indicated.

indicating that the latter protein essentially maintains the same overall folding properties (Supplementary Figure 2). The essential role of $Mia40_{3S-S}$ in the formation of the intersubunit disulfide bonds was shown through SDS-PAGE analysis (Supplementary Figure 2). The subsequent addition of 1 equiv of FAD produces major spectral changes and a $^{1}H-^{15}N$ HSQC map completely superimposable to that of the *E. coli*-purified sf-ALR state (Supplementary Figure 2). At the end of the maturation process, all three cysteine pairs (the structural, proximal, and intersubunit disulfides) of sf-ALR are involved in disulfide bonds, as monitored through NMR by analyzing their C$\beta$ chemical shifts, which are characteristic of the oxidation state of the cysteine residues.[26] In conclusion, the sequential addition of Mia40 and FAD forms the *E. coli*-purified covalent dimeric state of sf-ALR with all three disulfide bonds formed and FAD properly inserted in its binding pocket.

To address whether all three disulfide bonds are formed by Mia40 or whether FAD can have a role in their formation, we have analyzed the effect of the addition of 1 equiv of FAD only. It appears that addition of FAD determines the formation of the proximal disulfide, as monitored by $^{1}H/^{15}N$ chemical shifts of cysteine residues in a selectively labeled cysteine sample. Indeed, the NH cross-peak of Cys65, which forms the proximal disulfide bond with Cys62, has the typical chemical shift of its oxidized state, while the other Cys residues have chemical shifts typical of the fully reduced FAD-bound state (Figure 4). FAD

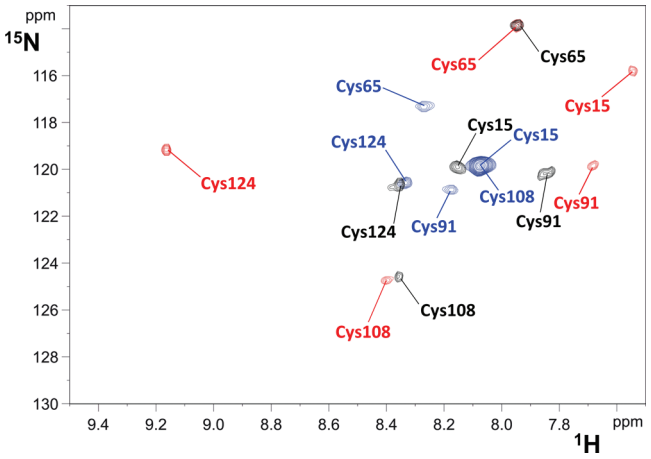


**Figure 4.** FAD-induced disulfide bond formation in the maturation process of sf-ALR. Overlay of $^{1}H-^{15}N$ HSQC spectra of ($^{13}C$,$^{15}N$) Cys-selectively labeled sf-ALR in its fully oxidized FAD-bound form (in red), in its fully reduced apo state (blue), and in the presence of 1 equiv of FAD (black). Direct comparison of the cysteine NH chemical shifts in their different redox state indicates that FAD induces only the formation of the proximal disulfide bond. Residue numbering refers to sf-ALR sequence.

addition thus induces only the formation of the proximal disulfide bond and, in the full maturation process of sf-ALR, Mia40 is responsible specifically for the formation of both the structural and intersubunit disulfide bonds.

To understand whether the processes of folding, oxidation, and maturation of ALR have a specific sequential order, reduced FAD-free sf-ALR was presented first with 1 equiv of FAD and then with 2 equiv of $Mia40_{3S-S}$. The $^{1}H-^{15}N$ HSQC map of sf-ALR upon FAD addition shows drastic chemical shift changes (Supplementary Figure 3), typical of a folded protein and similar to that of the *E. coli*-purified sf-ALR state. According to heteronuclear relaxation data, this FAD-bound protein state is dimeric ($\tau_m$ 12.2 ± 1.5 ns). However, SDS-PAGE analysis shows that FAD addition does not determine the formation of a covalent dimer that is formed only upon addition of $Mia40_{3S-S}$ (Supplementary Figure 4). The need of $Mia40_{3S-S}$ for the covalent dimerization of sf-ALR is consistent with the inability of reduced Mia40, *i.e.*, with a reduced catalytic CPC motif ($Mia40_{2S-S}$ hereafter) to form the covalent sf-ALR dimer (as assessed by nonreducing SDS-PAGE, Supplementary Figure 4). However, at variance with what was observed in the sequential addition of $Mia40_{3S-S}$ first followed by FAD, the $^{1}H-^{15}N$


dx.doi.org/10.1021/cb200485b | *ACS Chem. Biol.* 2012, 7, 707−714

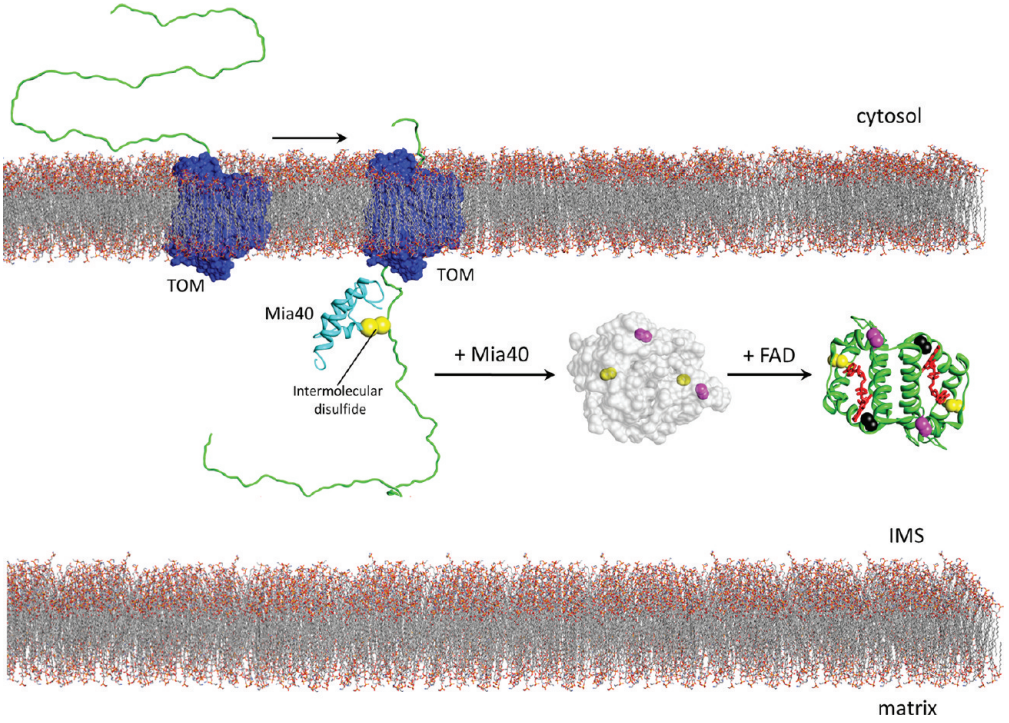


**Figure 5.** Mechanism of import and maturation of mitochondrial FAD-dependent sulfhydryl oxidase. Reduced, unfolded Erv1/ALR (in green) slips through the TOM pore (blue-colored) and is engaged with Mia40 (in cyano) through an intermolecular disulfide bond (yellow spheres). Then, upon Mia40 release, the structural disulfide bonds (yellow spheres on the gray surface of Erv1/ALR) are formed and a dimeric native-like, flexible state of Erv1/ALR (gray surface) is produced. In the case of ALR, two further molecules of Mia40 form the intersubunit disulfide bonds (magenta spheres on the gray surface of Erv1/ALR). In the final step, two FAD molecules (in red) bind to the FAD-binding domain of Erv1/ALR, producing both the oxidation of the proximal disulfide bond (black spheres on the green ribbon representation of Erv1/ALR) and the acquisition of a well-ordered, enzymatically active FAD-binding domain.

HSQC map of the final mixture (after addition of FAD and then of $Mia40_{3S-S}$) is very similar but not completely superimposable to that of the *E. coli*-purified sf-ALR state (Supplementary Figure 3). Also in this case, all of the cysteine residues in the final mixture are fully oxidized. The observed chemical shift variations ($\Delta\delta_{avg}$ = 0.09 ppm) between this covalent dimer and that obtained with a reverse order addition are located at the dimeric subunit interface and near the FAD binding pocket (Supplementary Figure 3). These results suggest the occurrence of local structural variations depending on whether FAD is inserted before or after Mia40-induced disulfide bridge formation, suggesting a slightly different orientation of the dimeric subunits and/or of the FAD moiety. These local structural variations have functional importance as they affect the electron transfer process to cytochrome *c*. ALR reconstituted by sequential additions of $Mia40_{3S-S}$ and FAD guarantees faster cyt *c* reduction and higher level of cyt *c* reduction than the reversed reconstitution procedure (Supplementary Figure 5).

**Molecular Mechanism of Import and Maturation of Erv1/ALR.** In this study import assays showed that the FAD-binding domain of Erv1/ALR is required and fully capable of translocation across the outer membrane and import into the IMS, while the N-terminal domain is dispensable for import in isolated mitochondria. Our studies on Erv1 mutants reveals that the previously reported[15,16] dependence of Erv1 import on Mia40 stems from the C-terminal segment of the FAD-binding domain. In particular, the deletion analysis narrowed down the absolutely minimal Erv1 segment for binding to Mia40 to the internal peptide sequence 134−176 of Erv1 (43 residues). This is the first experimental evidence for a "noncanonical" targeting signal for Erv1, which diverts from the identifiable internal targeting signals found in CHCH substrates.[27]

Mia40 oxidizes not only the strictly conserved structural disulfide but also the intersubunit disulfide (present in ALR and not in Erv1), which has a structural role in stabilizing the ALR dimer. However, it does not form the proximal disulfide that is induced by FAD. The Mia40 action specifically on the structural disulfide bonds is in agreement with the proposed general role of Mia40 in inducing the folding of its substrates[8] and also in line with its reported selectivity on cysteine binding of other substrates unrelated to Erv1/ALR.[7,24,28,29] However, unlike other Mia40 substrates, Erv1/ALR binds FAD, which together with the Mia40 action plays a key role in the protein maturation mechanism. Atomic resolution/NMR studies here defined the structural features of ALR in the presence or absence of Mia40 and FAD. We found that the fully reduced state of ALR, *i.e.*, before its interaction with Mia40 or FAD, is not completely unstructured but retains a large part of the native secondary structure and that Mia40-induced disulfide formation in ALR is not sufficient to freeze a unique conformational state of ALR, at variance with what occurs for other Mia40-substrate such as Cox17.[30] On the contrary, FAD has the foremost role to obtain a native-like conformation for ALR and also selectively oxidizes its proximal disulfide pair. With this type of substrate, the Mia40-induced disulfide formation process is not sufficient to produce a native-like rigid conformation and FAD binding is additionally required. This feature distinguishes ALR from the typical Mia40 substrates. Finally, these two binding events (Mia40-induced


dx.doi.org/10.1021/cb200485b | *ACS Chem. Biol.* 2012, 7, 707−714

oxidation and FAD binding) must occur in a strictly sequential manner to obtain a fully active ALR domain. We therefore suggest that the basic capacity of Mia40 to introduce one disulfide with concomitant localized folding of the substrate is common to all Mia40 substrates, but additional steps (such as the FAD binding here or other ligand binding in other proteins) may be needed for complete folding or maturation of different (more structurally complex) substrates.

This work has revealed that the Mia40-dependent mechanism of import and maturation of sulfydryl oxidases in the IMS depends on the fine-tuning and precise coordination of necessary and nonoverlapping events involving specific structural domains (Figure 5).

## METHODS

**Cloning of Erv1 and ALR.** For import experiments of Erv1, wild-type, Cys mutants, and ΔN72, ΔN133, ΔC13 deletions were cloned as *Bam*HI/*Eco*RI fragments in pSP64 vector for *in vitro* translation. In the case of ΔN133, five extra methionines were fused at its C-terminal end to boost the radioactive signal during *in vitro* translation in reticulocyte lysate.[10]

For the yeast complementation assays, Erv1 (wild-type and mutants) was subcloned from pSP64 into pRS316up40, which contains the up40 promoter of yeast Mia40.[13] Human ALR (wild-type and C154/C165A double mutant) was subcloned by PCR using as a template a pSP64 vector carrying these genes and oligonucleotides with the restriction enzyme sites XhoI (forward) and *Eco*RI (reverse). This XhoI/*Eco*RI cassette was then cloned as a downstream fusion to the DNA sequence encoding the first 1−85 amino acids of *S. cerevisiae* cytochrome b2 in the pRS316up40 yeast expression vector.

**Recombinant Protein Production and Characterization.** Mia40 and sf-ALR proteins were expressed in *Escherichia coli* BL21(DE3) gold cells (Stratagene) and purified following already described protocols.[7,13] The ($^{13}$C,$^{15}$N) Cys-selectively labeled sf-ALR was produced following the same procedure reported in Banci *et al.*[31] sf-ALR construct corresponds to the ALR isoform lacking the first 80 residues and contains the cysteine residues forming the proximal and both intersubunit and intrasubunit structural disulfides.

To completely unfold sf-ALR, the protein was precipitated in the presence of 20% (v/v) trichloroacetic acid and resuspended in 6 M guanidinium, 50 mM Tris, 150 mM NaCl, 0.5 mM EDTA, 100 mM DTT, pH 8. A PD-10 desalting column (Amersham Pharmacia Biosciences) was performed with the same buffer, to remove all free FAD molecules. Subsequently the protein was subjected to consecutive dialyses in 50 mM Tris, 150 mM NaCl, 0.5 mM EDTA, 100 mM DTT, pH 8 with decreasing amounts of urea starting with a concentration of 6 M down to 0 M. In the last step the protein was incubated with an additional amount of DTT (100 mM) and the previous buffer was exchanged with 50 mM phosphate buffer, 0.5 mM EDTA, pH 7 through another PD-10 desalting column in anaerobic conditions. After this procedure, the protein was completely reduced, as confirmed by a nonreducing SDS-PAGE in presence and in absence of 4-acetamido-4′-maleimidylstilbene-2,2′- disulfonic acid (AMS) (Supplementary Figure 1).

The aggregation state of different sf-ALR forms (sf-ALR, FAD-free sf-ALR and FAD-free sf-ALR in presence of 100 mM DTT) was investigated by analytical gel filtration chromatography and light scattering measurements. Protein samples of 100 μM concentration were run on a Superdex 200 HR-10/30 size exclusion column on AKTA-FPLC system (Amersham Pharmacia Biosciences) at a flow rate of 0.6 mL min$^{-1}$ connected with a multiangle light scattering (DAWN-EOS, Wyatt Technologies) coupled with quasielastic light scattering detectors. The system was previously equilibrated in 50 mM phosphate buffer, 0.5 mM EDTA, pH 7 with and without 100 mM DTT. Analytical gel filtration chromatography was conducted by equilibrating Superdex 75 HR 10/30 (Amersham Pharmacia Biotech) on a AKTA-FPLC system (Amersham Pharmacia Biosciences) with 50 mM phosphate buffer, 0.5 mM EDTA, pH 7 in the presence and absence of 100 mM DTT at a flow rate of 0.7 mL min$^{-1}$. The standards used for the calibration curve were conalbumin, carbonic anhydrase, ribonuclease, and aprotinin (Gel Filtration Calibration Kits LMW, GE Healthcare).

The cysteine redox state of Mia40, sf-ALR, and protein mixtures was investigated by a gel shift assay after modification with AMS. Each sample, with a final protein concentration of 40 μM, was treated with 1% (v/v) SDS and AMS in excess. The samples were incubated for 1 h at 37 °C and then subjected to nonreducing SDS-PAGE, which were stained with Coomassie Blue. AMS reacts with free thiol groups, resulting in a mobility shift of the protein on SDS-PAGE due to its increase in size of 0.5 kDa per AMS molecule.

CD spectra (190−260 nm) were recorded on a Jasco-810 spectropolarimeter on 20 μM protein solutions in 50 mM phosphate buffer, 0.5 mM EDTA, pH 7, at 25 °C. Each spectrum was obtained as the average of four scans and corrected by subtracting the contributions of the buffer. Quantitative estimate of the secondary structure contents was made by using the DICOPROT software package.

Reduction of human cytochrome *c* was followed through the change of the absorbance monitored at 550 nm in a UV−vis light spectrophotometer (Cary 50 spectrophotometer Varian). All samples were in phosphate buffer 50 mM, EDTA 0.5 mM, pH 7, in anaerobic conditions. Protein concentrations of fully reduced FAD-free sf-ALR, FAD, and oxidized cytochrome *c* were 30 μM, and that of Mia40$_{3S-S}$ was 60 μM.

***In Vivo* Yeast Complementation Assay.** For the yeast complementation experiments, the GalErv1 *S. cerevisiae* strain was transformed with the pRS316 plasmid (which confers uracil auxotrophy) carrying Erv1 (wild-type and mutants, in Figure 1b). The analysis was performed as described previously.[13]

**Import of Radiolabeled Precursors Erv1 in Yeast Mitochondria.** Wild-type Erv1 and mutants (C30/33S, C130/133S, C159/176S, C159S, C176S, ΔN72, ΔN133, ΔC13) were synthesized using the TNT SP6-coupled transcription/translation reticulocyte lysate kit (Promega) as $^{35}$S-labeled-precursors. Each radioactive precursor was imported in 50 μg of purified wild-type or Gal-Mia40 *S. cerevisiae* mitochondria in the presence of 2 mM ATP and 2.5 mM NADH or 2 mM Valinomycin (to deplete the membrane potential) for the indicated time points at 30 °C. The reactions were either left untreated or blocked with 25 mM *N*-ethylmaleimide (NEM, to reveal the intermediate with endogenous Mia40). Mitochondria were resuspended in 1.2 M sorbitol/20 mM Hepes pH 7.4, followed by a treatment with proteinase K (PK) or trypsin for 30 min on ice to remove unimported material. Phenylmethanesulfonyl fluoride (PMSF; 4 mM) or soybean trypsin inhibitor (SBTI; 1 mg mL$^{-1}$) was added to arrest the protease treatment. Finally, samples were resuspended in Laemmli sample buffer with or without β-mercaptoethanol as indicated and analyzed by SDS-PAGE. The results were visualized by digital autoradiography (Molecular Dynamics). Immunopreciapitation after import (Figure 1, lanes 14−16) was performed according to ref 27 using 100 μg of mitochondria for each immunoprecitation reaction.

**NMR Spectroscopy.** NMR experiments for resonance assignment were carried out on 0.5 mM ($^{13}$C,$^{15}$N)-labeled fully reduced FAD-free sf-ALR samples in 50 mM phosphate buffer, pH 7.0, containing 10% (v/v) $D_2O$. All NMR spectra were collected at 308 K, processed using the standard Bruker software (Topspin 1.3), and analyzed with the CARA program.[32] The $^{1}$H, $^{13}$C, and $^{15}$N backbone resonance assignment was performed following a standard protocol based on triple-resonance NMR experiments. Seventy-three of the 116 possible backbone amide peaks were observed in the $^{1}$H−$^{15}$N HSQC spectrum (63% of backbone detectability); 62% of these peaks were assigned and mainly belong to the N- and C- terminal tails and loops (residues 8−15, 34−37, 40, 42, 47−50, 57−59, 80−82, 86−87, 102−103, 109−125). The unassigned amide peaks are considerably broad (some of them experiencing double resonances) thus preventing the detection of their $^{13}C_\beta$ and, often, of $^{13}C_\alpha$ resonances in the triple resonance NMR spectra. Such NH broadening effect indicates the presence of conformational exchange processes in the unassigned regions. To

determine the secondary structure elements, chemical shift index analysis was performed by CSI[33] and PECAN[34] programs. Relaxation experiments on $^{15}$N-labeled samples were performed at a 600 MHz Bruker spectrometer measuring $^{15}$N backbone longitudinal ($R_1$) and transverse ($R_2$) relaxation rates and heteronuclear $^{15}$N{$^1$H}-NOEs.

The resonance assignment of the fully oxidized FAD-bound state of sf-ALR was already available[13] and deposited at the BioMagResBank database (accession number 18029).

To follow the maturation process by NMR, we produced $^{15}$N-labeled, ($^{13}$C,$^{15}$N)-labeled and ($^{13}$C,$^{15}$N)-selectively cysteine labeled samples of fully reduced FAD-free sf-ALR and checked their cysteine redox state by gel shift assay after protein AMS-modification. Then, these samples were titrated with unlabeled $Mia40_{3S-S}$ and FAD or *vice versa* at 308 K, following the reaction by two-dimensional $^1$H−$^{15}$N HSQC spectra. Triple resonance spectra were performed on the final protein mixtures to analyze the cysteine redox state through $^{13}C_\beta$ and $^{13}C_\alpha$ chemical shift values.[26] Gel shift assay of protein mixtures subjected to AMS-modification was also performed along the titration experiments (Supplementary Methods).

## ■ ASSOCIATED CONTENT

### Supporting Information

Cysteine redox and aggregation state of fully reduced FAD-free sf-ALR; maturation process of sf-ALR by sequential addition of $Mia40_{3S-S}$ and FAD and *vice versa*; nonreducing SDS-PAGE analysis of FAD and $Mia40_{3S-S}$/$Mia40_{2S-S}$ mixture; catalytic activity of the reconstituted sf-ALR enzyme; and $^{15}$N relaxation data of fully reduced FAD-free sf-ALR and of *E. coli*-purified sf-ALR This material is available free of charge *via* the Internet at http://pubs.acs.org.

## ■ AUTHOR INFORMATION

### Corresponding Author

*E-mail: tokatlid@imbb.forth.gr; banci@cerm.unifi.it; ivanobertini@cerm.unifi.it.

### Author Contributions

E.K., M.A., and P.K. produced constructs, performed import and complementation assays, and analyzed the data (all contributed equally); N.K. provided expert technical assistance; C.P. purified recombinant proteins; K.T., L.B., and I.B. planned the research, analyzed the data, and coordinated the writing of the text, to which all of the coauthors contributed; S.C.-B. planned and guided the flow of NMR experiments; C.C. and K.G. performed protein production and characterization for NMR samples; R. P. recorded the NMR spectra and analyzed the data.

### Notes

The authors declare no competing financial interest.

## ■ ACKNOWLEDGMENTS

This work was supported by the Access to Research Infrastructures activity in the seventh Framework Programme of the EC (Bio-NMR - Contract 261863) and by the Italian MIUR-FIRB PROTEOMICA-RBRN07BMCT (to I.B. and L.B.). Financial support from IMBB-FORTH, the University of Crete and the European Social Fund, and national resources (to K.T.) is gratefully acknowledged.

## ■ REFERENCES

(1) Deponte, M., and Hell, K. (2009) Disulphide bond formation in the intermembrane space of mitochondria. *J. Biochem. 146*, 599−608.
(2) Herrmann, J. M., and Riemer, J. (2010) The intermembrane space of mitochondria. *Antioxid. Redox. Signaling 13*, 1341−1358.
(3) Neupert, W., and Herrmann, J. M. (2007) Translocation of proteins into mitochondria. *Annu. Rev. Biochem. 76*, 723−749.
(4) Chacinska, A., Koehler, C. M., Milenkovic, D., Lithgow, T., and Pfanner, N. (2009) Importing mitochondrial proteins: machineries and mechanisms. *Cell 138*, 628−644.
(5) Sideris, D. P., and Tokatlidis, K. (2010) Oxidative protein folding in the mitochondrial intermembrane space. *Antioxid. Redox. Signaling 13*, 1189−1204.
(6) Mesecke, N., Terziyska, N., Kozany, C., Baumann, F., Neupert, W., Hell, K., and Herrmann, J. M. (2005) A disulfide relay system in the intermembrane space of mitochondria that mediates protein import. *Cell 121*, 1059−1069.
(7) Banci, L., Bertini, I., Cefaro, C., Ciofi-Baffoni, S., Gallo, A., Martinelli, M., Sideris, D. P., Katrakili, N., and Tokatlidis, K. (2009) MIA40 is an oxidoreductase that catalyzes oxidative protein folding in mitochondria. *Nat. Struct. Mol. Biol. 16*, 198−206.
(8) Banci, L., Bertini, I., Cefaro, C., Cenacchi, L., Ciofi-Baffoni, S., Felli, I. C., Gallo, A., Gonnelli, L., Luchinat, E., Sideris, D. P., and Tokatlidis, K. (2010) Molecular chaperone function of Mia40 triggers consecutive induced folding steps of the substrate in mitochondrial protein import. *Proc. Natl. Acad. Sci. U.S.A. 107*, 20190−20195.
(9) Ang, S. K., and Lu, H. (2009) Deciphering structural and functional roles of individual disulfide bonds of the mitochondrial sulfhydryl oxidase Erv1p. *J. Biol. Chem. 284*, 28754−28761.
(10) Lionaki, E., Aivaliotis, M., Pozidis, C., and Tokatlidis, K. (2010) The N-terminal shuttle domain of Erv1 determines the affinity for Mia40 and mediates electron transfer to the catalytic Erv1 core in yeast mitochondria. *Antioxid. Redox. Signaling 13*, 1327−1339.
(11) Bien, M., Longen, S., Wagener, N., Chwalla, I., Herrmann, J. M., and Riemer, J. (2010) Mitochondrial disulfide bond formation is driven by intersubunit electron transfer in Erv1 and proofread by glutathione. *Mol. Cell 37*, 516−528.
(12) Grumbt, B., Stroobant, V., Terziyska, N., Israel, L., and Hell, K. (2007) Functional characterization of Mia40p, the central component of the disulfide relay system of the mitochondrial intermembrane space. *J. Biol. Chem. 282*, 37461−37470.
(13) Banci, L., Bertini, I., Calderone, V., Cefaro, C., Ciofi-Baffoni, S., Gallo, A., Kallergi, E., Lionaki, E., Pozidis, C., and Tokatlidis, K. (2011) Molecular recognition and substrate mimicry drive the electron-transfer process between MIA40 and ALR. *Proc. Natl. Acad. Sci. U.S.A. 108*, 4811−4816.
(14) Daithankar, V. N., Farrell, S. R., and Thorpe, C. (2009) Augmenter of liver regeneration: substrate specificity of a flavin-dependent oxidoreductase from the mitochondrial intermembrane space. *Biochemistry 48*, 4828−4837.
(15) Terziyska, N., Grumbt, B., Bien, M., Neupert, W., Herrmann, J. M., and Hell, K. (2007) The sulfhydryl oxidase Erv1 is a substrate of the Mia40-dependent protein translocation pathway. *FEBS Lett. 581*, 1098−1102.
(16) Gabriel, K., Milenkovic, D., Chacinska, A., Muller, J., Guiard, B., Pfanner, N., and Meisinger, C. (2007) Novel mitochondrial intermembrane space proteins as substrates of the MIA import pathway. *J. Mol. Biol. 365*, 612−620.
(17) Daithankar, V. N., Schaefer, S. A., Dong, M., Bahnson, B. J., and Thorpe, C. (2010) Structure of the human sulfhydryl oxidase augmenter of liver regeneration and characterization of a human mutation causing an autosomal recessive myopathy. *Biochemistry 49*, 6737−6745.
(18) Endo, T., Yamano, K., and Kawano, S. (2010) Structural basis for the disulfide relay system in the mitochondrial intermembrane space. *Antioxid. Redox. Signaling 13*, 1359−1373.
(19) Banci, L., Bertini, I., Calderone, V., Cefaro, C., Ciofi-Baffoni, S., Gallo, A., and Tokatlidis, K. (2012) An electron transfer path through an extended disulfide relay system: the case of the redox protein ALR. *J. Am. Chem. Soc. 134*, 1442−1445.
(20) Lange, H., Lisowsky, T., Gerber, J., Muhlenhoff, U., Kispal, G., and Lill, R. (2001) An essential function of the mitochondrial sulfhydryl oxidase Erv1p/ALR in the maturation of cytosolic Fe/S proteins. *EMBO Rep. 2*, 715−720.

(21) Farrell, S. R., and Thorpe, C. (2005) Augmenter of liver regeneration: a flavin-dependent sulfhydryl oxidase with cytochrome c reductase activity. *Biochemistry 44*, 1532−1541.
(22) Muller, J. M., Milenkovic, D., Guiard, B., Pfanner, N., and Chacinska, A. (2008) Precursor oxidation by mia40 and erv1 promotes vectorial transport of proteins into the mitochondrial intermembrane space. *Mol. Biol. Cell 19*, 226−236.
(23) Hofhaus, G., Lee, J. E., Tews, I., Rosenberg, B., and Lisowsky, T. (2003) The N-terminal cysteine pair of yeast sulfhydryl oxidase Erv1p is essential for in vivo activity and interacts with the primary redox centre. *Eur. J. Biochem. 270*, 1528−1535.
(24) Sideris, D. P., and Tokatlidis, K. (2007) Oxidative folding of small Tims is mediated by site-specific docking onto Mia40 in the mitochondrial intermembrane space. *Mol. Microbiol. 65*, 1360−1373.
(25) Lu, H., Golovanov, A. P., Alcock, F., Grossmann, J. G., Allen, S., Lian, L. Y., and Tokatlidis, K. (2004) The structural basis of the TIM10 chaperone assembly. *J. Biol. Chem. 279*, 18959−18966.
(26) Sharma, D., and Rajarathnam, K. (2000) $^{13}$C NMR chemical shifts can predict disulfide bond formation. *J. Biomol. NMR 18*, 165−171.
(27) Sideris, D. P., Petrakis, N., Katrakili, N., Mikropoulou, D., Gallo, A., Ciofi-Baffoni, S., Banci, L., Bertini, I., and Tokatlidis, K. (2009) A novel intermembrane space-targeting signal docks cysteines onto Mia40 during mitochondrial oxidative folding. *J. Cell Biol. 187*, 1007−1022.
(28) Gross, D. P., Burgard, C. A., Reddehase, S., Leitch, J. M., Culotta, V. C., and Hell, K. (2011) Mitochondrial Ccs1 contains a structural disulfide bond crucial for the import of this unconventional substrate by the disulfide relay system. *Mol. Biol. Cell 22*, 3758−3767.
(29) Kloppel, C., Suzuki, Y., Kojer, K., Petrungaro, C., Longen, S., Fiedler, S., Keller, S., and Riemer, J. (2011) Mia40-dependent oxidation of cysteines in domain I of Ccs1 controls its distribution between mitochondria and the cytosol. *Mol. Biol. Cell 22*, 3749−3757.
(30) Banci, L., Bertini, I., Cefaro, C., Ciofi-Baffoni, S., and Gallo, A. (2011) Functional role of two interhelical disulfide bonds in human Cox17 protein from a structural perspective. *J. Biol. Chem. 286*, 34382−34390.
(31) Banci, L., Bertini, I., Ciofi-Baffoni, S., Hadjiloi, T., Martinelli, M., and Palumaa, P. (2008) Mitochondrial copper(I) transfer from Cox17 to Sco1 is coupled to electron transfer. *Proc. Natl. Acad. Sci. U.S.A. 105*, 6803−6808.
(32) Keller, R. (2004) *The Computer Aided Resonance Assignment Tutorial*, CANTINA Verlag, Goldau.
(33) Wishart, D. S., and Sykes, B. D. (1994) The $^{13}$C chemical shift index: a simple method for the identification of protein secondary structure using $^{13}$C chemical shift data. *J. Biomol. NMR 4*, 171−180.
(34) Eghbalnia, H. R., Wang, L., Bahrani, A., Assadi, A., and Markley, J. L. (2005) Protein energetic conformational analysis from NMR chemical shifts (PECAN) and its use in determining secondary structural elements. *J. Biomol. NMR 32*, 71−81.